NIH Public Access
Author Manuscript
Neuroimage. Author manuscript; available in PMC 2013 June 05.

Published in final edited form as:
Neuroimage. 2012 February 1; 59(3): 2670–2677. doi:10.1016/j.neuroimage.2011.08.052.

Deficient MWF mapping in multiple sclerosis using 3D whole-brain multi-component relaxation MRI

Hagen H. Kitzler[a,*,1], **Jason Su**[b,1], **Michael Zeineh**[b], **Cynthia Harper-Little**[c], **Andrew Leung**[d], **Marcelo Kremenchutzky**[e], **Sean C. Deoni**[f], and **Brian K. Rutt**[b]

[a]Department of Neuroadiology, University Hospital Carl Gustav Carus, Technische Universität Dresden, Fetscherstr. 74, 01307 Dresden, Germany

[b]Richard M. Lucas Center for Imaging, Radiology Department, Stanford University, 1201 Welch Rd, Stanford, CA 94305-5488, USA

[c]Imaging Research Laboratories, Robarts Research Institute, The University of Western Ontario, P.O. Box 5015 100 Perth Dr, London, ON, Canada N6A 5K8

[d]Department of Diagnostic Radiology and Nuclear Medicine, University Hospital, The University of Western Ontario, 339 Windermere Rd, London, ON, Canada N6A 5A5

[e]Department of Clinical Neurological Sciences, The University of Western Ontario, 339 Windermere Rd, London, ON, Canada N6A 5A5

[f]Division of Engineering, Brown University, 182 Hope St, Providence, RI 02912, USA

Abstract

Recent multiple sclerosis (MS) MRI research has highlighted the need to move beyond the lesion-centric view and to develop and validate new MR imaging strategies that quantify the invisible burden of disease in the brain and establish much more sensitive and specific surrogate markers of clinical disability. One of the most promising of such measures is myelin-selective MRI that allows the acquisition of myelin water fraction (MWF) maps, a parameter that is correlated to brain white matter (WM) myelination. The aim of our study was to apply the newest myelin-selective MRI method, multi-component Driven Equilibrium Single Pulse Observation of T1 and T2 (mcDESPOT) in a controlled clinical MS pilot trial. This study was designed to assess the capabilities of this new method to explain differences in disease course and degree of disability in subjects spanning a broad spectrum of MS disease severity. The whole-brain isotropically-resolved 3D acquisition capability of mcDESPOT allowed for the first time the registration of 3D MWF maps to standard space, and consequently a formalized voxel-based analysis of the data. This approach combined with image segmentation further allowed the derivation of new measures of MWF deficiency: total deficient MWF volume (DV) in WM, in WM lesions, in diffusely abnormal white matter and in normal appearing white matter (NAWM). Deficient MWF volume fraction (DVF) was derived from each of these by dividing by the corresponding region volume. Our results confirm that lesion burden does not correlate well with clinical disease activity measured with the extended disability status scale (EDSS) in MS patients. In contrast, our measurements of DVF in NAWM correlated significantly with the EDSS score ($R^2 = 0.37$; $p < 0.001$). The same quantity discriminated clinically isolated syndrome patients from a normal control population ($p < 0.001$) and discriminated relapsing–remitting from secondary-progressive patients ($p < 0.05$); hence this new technique may sense early disease-related myelin loss and

© 2011 Elsevier Inc. All rights reserved.

*Corresponding author at: Department of Neuroradiology, University Hospital Carl Gustav Carus, Technische Universität Dresden, Fetscherstr, 74, 01307 Dresden, Germany. Fax: +49 351 458 4370.

[1]Both authors contributed equally to this work.

NIH-PA Author Manuscript
NIH-PA Author Manuscript
NIH-PA Author Manuscript

NIH-PA Author Manuscript

NIH-PA Author Manuscript

NIH-PA Author Manuscript

transitions to progressive disease. Multivariate analysis revealed that global atrophy, mean whole-brain myelin water fraction and white matter atrophy were the three most important image-derived parameters for predicting clinical disability (EDSS). Overall, our results demonstrate that mcDESPOT-defined measurements in NAWM show great promise as imaging markers of global clinical disease activity in MS. Further investigation will determine if this measure can serve as a risk factor for the conversion into definite MS and for the secondary transition into irreversible disease progression.

Keywords

Multiple sclerosis; Normal appearing white matter; Quantitative relaxation MRI; Myelin water fraction; Deficient MWF

Introduction

Multiple sclerosis and conventional MRI

Multiple sclerosis (MS), one of the most common disabling neurological diseases in young adults, is an immune-mediated disease that is poorly understood but is known to involve both demyelination and axonal destruction within the human central nervous system (CNS) (Platten et al., 2005). The pathology findings are heterogeneous but white matter (WM) demyelination is the recognized hallmark of the disease (Lucchinetti et al., 2000).

Conventional T1- and T2-weighted magnetic resonance imaging (MRI) studies reveal focal signal abnormalities, traditionally called lesions or “plaques”, throughout white matter (WM), and less frequently also gray matter (GM), in brain and spinal cord. In fact conventional MRI has revolutionized MS clinical practice (Vellinga et al., 2009), but it does not adequately fulfill the role of a disease biomarker. While MRI derived lesion count and volumetric measures are currently used as paraclinical markers in standardized diagnostic schemes (Polman et al., 2005), the lesion-centric view has been challenged by several studies revealing weak or non-significant correlations (Daumer et al., 2009; Fulton et al., 1999; Zivadinov, 2009). Presently available technologies have failed to meet the critical goal of reflecting MS patient disability status and predicting disease progression (Held et al., 2005; Sormani et al., 2003). When subjected to rigorous statistical analysis, conventional MRI measures appear to offer no more valid endpoint than that already offered by clinical measures of MS disability such as the extended disability status scale (EDSS) and the relapse rate (Daumer et al., 2009).

Quantitative MRI and imaging myelin in vivo

Newly developed quantitative MRI technologies have shown sensitivity to myelination and axonal integrity. They have been indicative of a process of diffusemyelin damage and axonal loss inMS not restricted to lesion tissue, but throughout the entire CNS parenchyma (Seewann et al., 2009; Vrenken et al., 2010).

Within the battery of newly developed quantitative MRI technologies, magnetization transfer imaging (MTI), (Filippi and Agosta, 2007; Horsfield, 2005) diffusion tensor imaging (DTI), (Schmierer et al., 2007; Song et al., 2003) and relaxation imaging (Karampekios et al., 2005; Papanikolaou et al., 2004) are all thought to provide information related to myelin content. However, measures derived from these approaches are non-specific with regard to demyelination. While quantitative MTI provides an estimate of the macromolecule-bound water fraction, this measure may also reflect other inflammation processes in MS (Gareau et al., 2000; Vavasour et al., 1998). A histological analysis

NIH-PA Author Manuscript

NIH-PA Author Manuscript

NIH-PA Author Manuscript

revealed a higher correlation between MTI measures and axonal density than myelin density in MS lesions (van Waesberghe et al., 1999). MTI measures therefore are considered to reflect an overall loss of membrane integrity, including demyelination (Dousset et al., 1995).

For DTI, significant fractional anisotropy is observed even in non-myelinated axonal nerve tissue (Beaulieu, 2002). More importantly, fractional anisotropy is low in regions of crossing fibers independent of myelin content (Oouchi et al., 2007).

With regards to single-component relaxation imaging, while both T1 and T2 relaxation times may be sensitive to myelin content, these are also influenced by additional factors including free water content and the presence of paramagnetic species such as iron.

Currently, T2 multi-component relaxation imaging (MCRI) provides the most established and specific means of quantifying myelin tissue content in vivo. In conventional T2 MCRI, multiple spin-echo images acquired over a range of echo times and multi-exponential data analysis are used to decompose the signal into water pools with a distribution of T2 times. Ultimately, this distribution is separated into main two pools: one intra- and extra-cellular water pool and a second “myelin water” pool, assumed to be trapped between the hydrophobic bilayers of the myelin sheath (Menon and Allen, 1991; Whittall et al., 1997). This is the quantity that links T2 MCRI and the technique that we employ. The myelin water fraction estimate derived this way shows strong correlation with histological assessment of myelin fraction (Laule et al., 2006; MacKay et al., 2009; Webb et al., 2003). For this reason, MCRI has become the de facto standard for non-invasive myelin quantification. Unfortunately, established MCRI methods require lengthy imaging times while providing limited volume coverage. For example, the multi-echo T2 relaxation method requires approximately 25 min to acquire a single slice with a voxel volume of 8.8 mm^3 (Madler et al., 2008; Whittall et al., 1997). There have been some recent improvements (Oh et al., 2007), however the volume coverage, spatial resolution, and imaging time characteristics of these methods make high resolution, whole-brain investigations challenging or impossible.

Multi-component DESPOT: a new MCRI method for myelin imaging

Multi-component driven equilibrium single pulse observation of T1/T2 (mcDESPOT) is the most recent MCRI technique that allows rapid acquisition of high-resolution whole-brain data which is then processed to yield quantitative two-pool parameters including myelin water fraction maps. Series of spoiled gradient echo (SPGR) and balanced steady-state free precession (bSSFP) scans are each collected over a range of flip angles (FA) at constant repetition times (TR). This data set allows reliable estimation of the relaxation properties of a two-pool model undergoing exchange at every voxel over the whole brain (Deoni et al., 2008b). One of the parameters is the fraction of water in the fast relaxing pool, which we have named the myelin water fraction (MWF) because of its similarity with the one defined by previous MCRI methods (Kolind and Deoni, 2011). We have further hypothesized that MWF derived from mcDESPOT will correlate directly with tissue myelin fraction (Deoni, 2009a,b) as have previous measures (Laule et al., 2006; MacKay et al., 2009).

The objectives of our study were (1) to derive MWF maps and a novel MWF-derived quantity that we term deficient MWF volume fraction (DVF) using mcDESPOT acquisitions from a broad spectrum of MS patients, (2) to test the hypothesis that MWF and/or DVF correlate with disability in MS and thus reflect non-lesional MS pathology that may determine disease severity, and (3) to assess the relative contributions of quantitative myelin-specific parameters and brain atrophy measures such as brain parenchymal volume fraction (PVF).

NIH-PA Author Manuscript

NIH-PA Author Manuscript

NIH-PA Author Manuscript

A novel and clearly advantageous feature of the mcDESPOT technique is that it efficiently covers the entire brain, producing isotropic and high quality datasets of the presumed MWF. This allows myelin quantification to be done much more rigorously, for the first time, using standard space approaches which have proven useful for other analyses such as voxel-based morphometry (Mechelli et al., 2005). In this study, we used these tools with mcDESPOT to conduct formalized correlations and group comparisons of myelin water fraction and atrophy measures with clinical disability.

Materials and methods

MS patients and healthy controls

All participants were recruited in conformance with local ethics board requirements of the University of Western Ontario, London, ON, Canada. The 26 patient cohort assembled for this controlled study was distributed across the different definite MS and pre-MS categories. There were 16 patients with definite MS: 5 relapsing–remitting (RRMS), 6 secondary-progressive (SPMS), and 5 primary-progressive (PPMS). In addition, 10 clinically isolated syndrome (CIS) patients were recruited. In all patients, the MS extended disability status scale (EDSS) was acquired. EDSS is an average score derived from measures of various functions of the central nervous system, using a scale from 0 to 10, with 10 representing greatest disability (Kurtzke, 1983). The median EDSS score for the patient group was 3.0 (max 7.5; min 0; IQR 4.5), with a median patient disease duration of 11 years (max 38.4 years, min 0.3 years; IQR 18 years). The disease duration was defined as the time between the onset of neurological symptoms and the MRI data acquisition. EDSS was acquired immediately on or shortly before the study MRI date. Within the entire group of patients, only 2 patients received immune modulating treatment: one CIS with Copaxone and one SPMS with Avonex. We also scanned a group of 26 healthy controls to be used for statistical comparison. The patient and control populations were indistinguishable by age according to a rank sum test at the 5% significance level. See Table 1 for more demographic data.

MRI data acquisition

Images were acquired with a clinical 1.5 T MRI scanner (GE Signa HDx, General Electric Healthcare, Waukesha, WI) and an 8-channel receive-only radio-frequency (RF) brain array coil. We acquired nearly isotropic [1.7 × 1.7 × 2.0 mm] whole-brain mcDESPOT data using the following imaging parameters: FOV = 22 cm, matrix = 128 × 128, slice thickness = 2 mm; SPGR parameters: echo time/repetition time (TE/TR) = 2.1/6.7 ms, flip angle (α)=[3, 4, 5, 6, 7, 8, 11, 13, 18]°; bSSFP parameters: TE/TR = 1.8/3.6 ms, α = [11, 14, 20, 24, 28, 34, 41, 51, 67]°, two phase cycles acquired per bSSFP flip angle. This protocol was consistent with the DESPOT-FM method, which accounts for errors due to B0 inhomogeneity (Deoni, 2009a). B1 inhomogeneity is small at 1.5 T so it was ignored. The total mcDESPOT acquisition time was ~13 min. For anatomical reference and lesional tissue analysis, additional 2D T2-FLAIR (TE/TR = 125/8800 ms, TI = 2200 ms, FOV = 22 cm, matrix = 256 × 256, slice thickness = 3 mm, whole-brain coverage in ~8 min) and 3D T1-MPRAGE (TE/TR = 3.8/9 ms, TI = 600 ms, FOV = 24 cm, matrix = 256 × 256, slice thickness = 1.2 mm, whole brain coverage in ~8 min) sequences were acquired.

MRI data postprocessing

All post-processing was accomplished using in-house Python scripts to automate usage of the FMRIB Software Library (FSL). First, we performed brain extraction (Smith and Jenkinson, 2000) and intra-subject linear co-registration of scans to a chosen mcDESPOT target image, SPGR α = 18° (Smith et al., 2004). The registered images were then processed with the mcDESPOT fitting code, which estimates the two-compartment model parameters

NIH-PA Author Manuscript

NIH-PA Author Manuscript

NIH-PA Author Manuscript

(Deoni et al., 2008a). We focused our analysis in this paper on MWF because of its particular relevance to MS.

All MWF maps were non-linearly registered to the MNI152 1 mm^3 isotropic resolution standard brain (International Consortium for Brain Mapping standard template) by first registering mcDESPOT target images using FSL's FNIRT with a warp resolution of 8 mm^3 and applying the resulting transforms to the maps. Subsequently, mean and standard deviation volumes were computed from the healthy controls' MWF maps. On a patient-by-patient basis, the MWF value at each voxel was compared to the healthy control distribution mean and standard deviation to produce a z-score value for that location. The resulting z-score maps were then transformed back from standard space to patient space with trilinear interpolation. Voxels that fell in the range of z-score <-4, i.e. that had a MWF at least 4 standard deviations below the mean healthy control value, were marked and defined as *deficient*. This choice of z-score <-4 means that we are looking at abnormalities in MWF that occur in <0.01% of the normal population and has been used in prior studies (Deoni, 2009b). These voxels were summed and scaled by the voxel volume to produce a measure of *deficient MWF volume* (DV) for each tissue region and patient. We then computed the fraction of a given region that was deficient by normalizing by the region volume. This latter measure was selected as the main outcome measure derived from our mcDESPOT approach and is termed the *deficient MWF volume fraction* (DVF). This measure was computed for both MS patients and healthy controls in each region.

Tissue region segmentation

The conventional MRI data were used to segment the tissue regions. Brains were segmented into gray matter (GM), WM and cerebrospinal fluid (CSF) with the T1-weighted MPRAGE data and the Statistical Parametric Mapping software package (SPM8; Wellcome Department of Imaging Neuroscience, UCL, London, UK) (Ashburner and Friston, 2005). The probabilistic maps were converted into binary masks by first median filtering with a $3 \times 3 \times 3$ voxel kernel to reduce errors due to noise in the images and then thresholding at the 0.5 level. A trained neuroradiologist edited the resulting WM masks and all voxels below the pontine level were excluded to standardize the analyzed brain parenchyma. Manual correction was applied to exclude false positively selected areas based on neuro-anatomical considerations. Special care was taken to fill in lesions on the WM masks and to exclude areas too close to CSF.

MS lesions were identified as well-defined focal areas of elevated MRI signal intensity in the FLAIR data. Lesions that were not bright on T2-FLAIR were not included. We applied a semi-automatic segmentation approach similar to the process used to derive areas of deficiency from MWF maps. Briefly, the FLAIR volume was warped to standard space using the previously calculated non-linear transform. Voxel-wise mean and standard deviation maps for healthy control subjects were calculated on the basis of FLAIR signal intensity. Since conventional MRI images have arbitrary intensity scales with intensity values that depend on various acquisition factors, a common scale was established by dividing all voxel intensities by the “robust maximum” (the signal value at the 98th percentile) in each skull-extracted FLAIR brain for healthy controls and patients. With this correction, we computed z-score maps for each MS patient and lesions were identified as voxels whose intensities were elevated 4 standard deviations above those in the control population. An experienced neuroradiologist edited these lesions masks, eliminating any voxels in non-brain tissue, at the brain surface, and intra-ventricular locations. The ITK-Snap software package (Yushkevich et al., 2006) provided a 3D seeding function to select and eliminate spurious voxel clusters. This approach enabled us to produce accurate masks of well-defined WM T2 lesions.

NIH-PA Author Manuscript

NIH-PA Author Manuscript

NIH-PA Author Manuscript

In a second step, regions of intermediate T2 signal intensity between those of focal lesions and WM, called *diffusely abnormal white matter* (DAWM) (Fazekas et al., 1999) were segmented. Using the same FLAIR-based z-score maps, masks were created with a threshold of z-score >+2. For each patient, selected areas in this resulting mask were compared against the previously defined lesion masks using MATLAB (MathWorks, Natick, MA, USA). Those 3D regions that contained a lesion were kept as lesion-surrounding DAWM, the rest were rejected (Fig. 1).

Finally, *normal appearing white matter* (NAWM) was defined as all WM voxels minus lesion and DAWM voxels (NAWM = WM − lesion − DAWM) for each patient (Fig. 1).

With all the segmentations complete, the WM, NAWM, DAWM, and T2 lesion masks were aligned to each subject's MWF map using nearest neighbor interpolation and transformations from the linear registration of the FLAIR and MPRAGE scans to the mcDESPOT target image. This enabled patient- and region-specific extraction of mean MWF and DVF. Fig. 2 shows a workflow schematic diagram for all of the above-described data post-processing.

Brain volume measurements

The parenchymal volume fraction (PVF), defined as the GM + WM (brain parenchymal) volume divided by the space inside the outer brain contour, is a measure of global atrophy (Kalkers et al., 2002). We computed PVF for each subject using FSL and MATLAB. Additionally, we derived volume measures for each of the tissue regions of interest, i.e. WM, NAWM, DAWM, and lesions, normalized by the subject's intracranial volume. These volume fractions provided standardized atrophy measures and a detailed picture of the volumetric state of each brain.

Voxel-based statistical analysis

Using the mean MWF and DVF scores for each WM tissue region and each subject, we performed a battery of Wilcoxon rank-sum tests to examine the ability of these measures to differentiate between healthy controls and different MS courses. We also examined the correlation between several of the derived quantities and EDSS, using both Pearson and Spearman correlations. We focused our attention on the most strongly correlated and interesting of these quantities: PVF, the logarithm of DVF in NAWM, and T2 lesion load.

Multiple linear regression (MLR) methods were applied to examine the ability of multiple image-derived quantities to predict EDSS. We used Mallows' Cp as the criterion for selection of the best MLR model (Mallows, 1973) that most parsimoniously explains the outcome. Using the R software environment (R Foundation for Statistical Computing, Vienna, Austria), an exhaustive search was conducted for all possible combinations of the following predictors: PVF, log(DVF) in whole brain, log(DVF) in WM, log(DVF) in NAWM, log(DVF) in lesions, log(DV) in these same four regions, mean MWF in those four regions, the volumes of those four regions (with lesion volume being the same as T2 lesion load), and the volume fractions of those four regions. This constituted a total of 21 possible predictors. F-tests were used to determine if each of the variables chosen in the best MLR model made a significant improvement over a model without it.

Results

Myelin water fraction analyses

The mean myelin water fraction was compared in different white matter regions between MS patients and healthy controls. Table 2 and Fig. 3 show that MWF values found in whole

NIH-PA Author Manuscript

NIH-PA Author Manuscript

NIH-PA Author Manuscript

brain normal WM (mean 0.192; SD 0.015) are higher than those derived from regions of interest using T2 MCRI (0.085–0.112) (Madler et al., 2008; Oh et al., 2006; Whittall et al., 1997). For each patient category, the mean MWF in various WM regions was compared to MWF in WM for healthy controls using Wilcoxon rank sum testing. This showed that for SPMS and PPMS patients, but not for CIS or RRMS patients, mean MWF in both total WM ($p<0.01$) and NAWM ($p<0.01$) was significantly lower than the corresponding mean WM MWF for healthy controls. Across all MS courses, the mean MWF value was significantly lower in DAWM and lesions than in WM of controls, as expected given the fundamental definition of MS as a focal demyelinating disease. We were not able to discriminate between the different MS courses using mean MWF values in T2 lesions, DAWM, NAWM or total WM. In spite of the generally monotonic downward trend of MWF with disease severity for all of the tissue regions, there were no significant differences in MWF between adjacent disease categories. No statistically significant difference was found between male and female control groups for mean MWF in WM ($p = 0.445$).

Deficient MWF volume fraction

Deficient voxels were identified from the MWF fraction map with the procedures described above. The pattern of such voxels substantially differed from the conventional T2 lesion mask (Fig. 1). Importantly, there were non-deficient voxels within lesions and deficient voxels extending substantially outside of lesions into DAWM and NAWM. This suggests that this novel measure not only characterizes the heterogeneity of lesion myelination but is also sensitive to the invisible burden of disease.

Table 2 shows DVF (total volume of deficient voxels within a region divided by the region volume) in different white matter regions for both MS patients and healthy controls. DVF was found to be approximately equal for CIS and RRMS courses. Progressive MS patients revealed an order of magnitude higher DVF in total WM compared to non-progressive patients. Interestingly, from RRMS to SPMS a ten-fold increase is seen in NAWM, contrasted by only a small difference in DVF between these two disease courses for DAWM or T2 lesions. Finally, a general increase in DVF was seen moving from NAWM to DAWM to T2 lesions as one would expect.

Rank sum testing of DVF in NAWM revealed that all patient classes could be distinguished from healthy controls with $p < 0.001$. RRMS patients had significantly lower DVF in both total WM and NAWM than SPMS patients with $p < 0.05$. This last observation contrasts with the same comparison using mean MWF, in which case no such significant differences were found (Fig. 4).

Parenchymal volume fraction

A similar series of significance tests was performed using the parenchymal volume fraction (PVF) atrophy measure. Unlike DVF, PVF fails to distinguish CIS ($p = 0.68$) and RRMS patients ($p = 0.76$) from healthy controls. In contrast, progressive SPMS and PPMS patients had significantly lower PVF than normals with $p < 0.01$. The PVF of SPMS patients was found to be lower than that of RRMS patients with $p<0.01$.

Correlation analyses

Simple (Pearson) linear regression of T2 lesion load (total volume of T2 lesions) against the clinical MS disability score EDSS revealed the expected low correlation ($R^2 = 0.28$, $p < 0.01$), reflecting its known poor predictive value of disease related disability (Fig. 5a). In contrast, DVF within NAWM, after a log transform, revealed a higher Pearson correlation to EDSS ($R^2 = 0.37$, $p < 0.001$), suggesting a more direct association to clinical impairment (Fig. 5b). In this cohort, PVF showed the strongest correlation to EDSS among the MRI-

NIH-PA Author Manuscript

NIH-PA Author Manuscript

NIH-PA Author Manuscript

derived parameters studied ($R^2 = 0.56$, $p < 0.0001$). This confirms the known association of brain atrophy with functional decline (Fig. 5c) (Kalkers et al., 2002; Rudick et al., 1999).

Repeating the correlation analysis with the Spearman rank correlation coefficient (which measures the monotonic but perhaps non-linear relationship between two variables), the lowest correlation was found between T2 lesion load and EDSS ($r_s = 0.49$; $p = 0.012$), a higher correlation with DVF in NAWM ($r_s = 0.60$; $p = 0.0012$) again, and the highest correlation with PVF ($r_s = -0.73$; $p < 0.0001$).

Multiple linear regression

A preferable method to predict EDSS is to incorporate multiple predictors rather than just one. The best MLR model for EDSS with the lowest Mallows' Cp among all possible combinations of only image-derived variables was the one that contained brain PVF ($p < 0.001$), mean whole brain MWF ($p < 0.001$), and the total WM volume fraction ($p < 0.01$). P-values were derived from F-tests which indicated that whole-brain MWF and WM volume fraction significantly improved the prediction of EDSS over that produced by PVF alone. This model explained 76% of the variance in EDSS (i.e. $R^2 = 0.76$, or adjusted $R^2 = 0.73$ after accounting for multiple predictors). If disease duration, age, and gender are included as non-imaging covariates, the best model was found to contain disease duration, PVF, and the volume fraction of DAWM ($R^2 = 0.82$, adjusted $R^2 = 0.79$), closely followed by models that included disease duration, PVF and either the volume of DAWM or the mean MWF of lesions.

Discussion

In this study, we have demonstrated that myelin-selective mcDESPOT allows the assessment of whole-brain myelin water fraction in MS patients and healthy controls at high isotropic spatial resolution and in clinically relevant scan times. This enabled the quantification of deficient MWF at both the single-voxel and region level using standard space voxel-based analysis (VBA). This allowed us to use formalized statistics for group comparison, which has not been possible with other quantitative myelin-selective MRI techniques to date. In traditional quantitative MRI analysis, parameters are measured by drawing regions of interest (ROIs) on images or quantitative maps. However, Meyers et al. have recently shown that voxel-based multi-component relaxation analysis is more consistent for extracting MWF information than standard ROI approaches in scan-rescan reproducibility experiments (Meyers et al., 2009). The principal advantage of using a standard space is that it allows every location in the brain to become a point of comparison between healthy and diseased subjects. This preserves spatial information and allows the detection of subtle disease-induced brain tissue changes independent of individual neuroanatomical variations.

An important quality metric of any quantitative MRI measurement is its variability. We found intersubject variability for mcDESPOT-derived mean total WM MWF among normals to be low, with a standard deviation of 0.015 (7.81% of the mean normal WM MWF). This is comparable to or better than the standard deviation in MWF derived from T2 MCRI (0.015–0.036) (Vavasour et al., 2006).

Another distinctive feature of our work is that we applied a novel semi-automatic strategy to segment MS lesions and to define important WM regions. The use of standard-space and a predefined z-score threshold to determine FLAIR hyperintensities led to semiautomatic, reliable and bias-free lesion and DAWM segmentations.

NIH-PA Author Manuscript

NIH-PA Author Manuscript

NIH-PA Author Manuscript

We sought to determine the extent of MWF abnormality, especially in NAWM but also in DAWM and lesions, across different courses of MS. Our analysis of the traditional MS surrogate marker, T2 lesion volume, confirms the known poor correlation with clinical disease activity in MS patients. The EDSS correlation results imply that brain atrophy and the NAWM burden of disease are better predictors of disability. It is known from previous studies that brain atrophy (PVF) correlates with EDSS, although the strength of this correlation has ranged from weak to moderate (Furby et al., 2008; Kalkers et al., 2002; Martola et al., 2007, 2010; Rudick et al., 2009). However, our work is the first to show that a quantitative myelin water fraction measure derived from mcDESPOT acquisition adds statistically significant patient disability predictive value on top of PVF, as evidenced by its inclusion in the optimal multiple linear regression model.

Previous papers have examined MWF in NAWM of MS patients but not in whole brain and not with a clear treatment of DAWM (Laule et al., 2004; Oh et al., 2007). We observed similar drops of mean MWF in NAWM and lesions compared to control WM as did T2 MCRI studies (Laule et al., 2004): about a 7.4% and 53.2% decrease vs. 16% and 52%. MWF values are generally larger with mcDESPOT compared to their T2 MCRI counterparts. There is speculation that this may be caused by the two-pool model of mcDESPOT or magnetization transfer effects (Deoni, 2011) but further study is required.

Careful multivariate model selection and statistical analyses were applied to the data. Exhaustive search was used to avoid the pitfalls of search methods like stepwise regression, which are prone to finding local minima rather than the global optimum (Korteweg et al., 2009). We derived a model for EDSS based on imaging-derived measures using PVF, whole brain mean MWF, and the volume fraction of white matter. One might describe these quantities as representing the overall brain atrophy, a quantification of the diffuse disease, and the atrophy of WM, which is the primary brain tissue affected by MS. A larger study will be needed to confirm whether these particular parameters remain the strongest predictors of clinical disability.

Measurements of deficient MWF volume fraction in NAWM robustly discriminated CIS-patients from a control population. This highly significant difference represents an important finding of our study, and contrasts with other quantitative imaging metrics including mean MWF which do not show the same sensitivity to early MS. This fact in particular demonstrates the potentially high sensitivity of mcDESPOT in detecting early and conventionally invisible disease-related myelin loss. Further longitudinal investigation will be needed to determine if this measure will serve as a risk factor for conversion into definite MS.

We found that this measure also discriminated patients with a relapsing–remitting course from secondary-progressive MS patients. This was also true for the atrophy measure PVF, but was not true for mean MWF. These findings suggest that the DVF and PVF metrics have merit in predicting conversion into secondary progressive MS. We speculate that the very large dynamic range of DVF will provide greater sensitivity to disease progression than PVF.

Notably, not all lesion tissue is considered deficient in MWF according to our definition (z-score <-4). This is in agreement with previous findings using T2MCRI,which showed that lesions had a heterogeneous MWF that perhaps reflects different stages of demyelination (Oh et al., 2007). Still, these areas have low MWF with a mean of 0.105, 41.1% below the mean in NAWM. Lesions can exhibit multiple component signal behavior. It remains to be determined if there is any substantial bias due to mcDESPOT's two-pool model.

NIH-PA Author Manuscript

NIH-PA Author Manuscript

NIH-PA Author Manuscript

Our results show that mcDESPOT is sensitive to brain tissue changes even at the pre-MS stage, well before established volumetric measures register significant changes. Brain volume loss is an established clinical marker in MS, however mcDESPOT-derived deficient MWF analysis provides more specific and spatially resolved information. These maps can be used to reveal particular regions of the brain that are affected by the disease. In our study, this spatially resolved information was collapsed into a single mean MWF or DVF quantity per region. A more detailed region-specific analysis remains as a future avenue of exploration, especially since it is known that certain WM structures are particularly vulnerable to the MS disease process.

Conclusions

The mcDESPOT method reveals an ordinarily hidden relationship between multiple sclerosis and the subtle micro-structural changes that are occurring in brain tissue well before lesions can be detected with conventional MRI. Furthermore, mcDESPOT-derived MWF targets, quantifies, and visualizes the principal substrate of disability in MS. The development and validation of this new MRI method is expected to yield better prognostic markers of disease progression in future MS studies.

The current state-of-the-art treatments are disease-modifying agents that at present are able to decrease relapse rates by 30% (Weiner, 2009). However, despite these advances, the field of MS still lacks specific markers to predict clinical relapses and disease progression. Novel immunotherapies and remyelinating therapeutic approaches are on the rise, but to date non-invasive technologies have failed to provide accurate, reliable tools to assess the state of myelination. Such methods are particularly needed for testing drug efficacy or for monitoring treatment. Quantitative myelin-selective imaging methods such as mcDESPOT will be extremely important for the investigation of in vivo, real time changes that occur within the CNS over the broad spectrum of natural MS courses as well as during treatment.

Acknowledgments

The authors would like to thank all of the study participants and their families, as well as our research support staff; in particular Donna Greer for patient recruitment. This work was supported by the Canadian Institutes of Health [MOP-8371]; the London Health Sciences Centre-General Electrics (LHSC-GE) Alliance Fund [Radiology Research Academic Fellowship]; and University of Western Ontario Academic Development Fund.

Abbreviations

CIS	clinically isolated syndrome
MCRI	multi-component relaxation imaging
MWF	myelin water fraction
DV	deficient MWF volume
DVF	deficient MWF volume fraction
NAWM	normal appearing white matter
DAWM	diffusely abnormal white matter
EDSS	extended disability status scale

References

Ashburner J, Friston KJ. Unified segmentation. NeuroImage. 2005 Jul 1; 26(3):839–851. [PubMed: 15955494]

NIH-PA Author Manuscript

NIH-PA Author Manuscript

NIH-PA Author Manuscript

Beaulieu C. The basis of anisotropic water diffusion in the nervous system — a technical review. NMR Biomed. 2002 Nov-Dec;15(7–8):435–455. [PubMed: 12489094]

Daumer M, Neuhaus A, Morrissey S, Hintzen R, Ebers GC. MRI as an outcome in multiple sclerosis clinical trials. Neurology. 2009 Feb 24; 72(8):705–711. [PubMed: 19073945]

Deoni SC. Transverse relaxation time (T2) mapping in the brain with off-resonance correction using phase-cycled steady-state free precession imaging. J. Magn. Reson. Imaging: JMRI. 2009a Aug; 30(2):411–417.

Deoni SC. Whole-brain Voxel-wise Analysis of Myelin Water Volume Fraction in Multiple Sclerosis. Proceedings of the ISMRM. 2009b; 17:344.

Deoni SC. Correction of main and transmit magnetic field (B0 and B1) inhomogeneity effects in multicomponent-driven equilibrium single-pulse observation of T1 and T2. Magn. Reson.Med.: off.j.Soc. Magn. Reson.Med./Soc.Magn. Reson.Med. 2011 Apr; 65(4):1021–1035.

Deoni SC, Rutt BK, Arun T, Pierpaoli C, Jones DK. Gleaning multicomponent T1 and T2 information from steady-state imaging data. Magn. Reson. Med. 2008a Dec; 60(6):1372–1387. [PubMed: 19025904]

Deoni SC, Rutt BK, Jones DK. Investigating exchange and multicomponent relaxation in fully-balanced steady-state free precession imaging. J. Magn. Reson. Imaging. 2008b Jun; 27(6):1421–1429. [PubMed: 18504765]

Dousset V, Brochet B, Vital A, Gross C, Benazzouz A, Boullerne A, et al. Lysolecithin-induced demyelination in primates: preliminary in vivo study with MR and magnetization transfer. AJNR Am. J. Neuroradiol. 1995 Feb; 16(2):225–231. [PubMed: 7726066]

Fazekas F, Barkhof F, Filippi M, Grossman RI, Li DK, McDonald WI, et al. The contribution ofmagnetic resonance imaging to the diagnosis ofmultiple sclerosis. Neurology. 1999 Aug 11; 53(3):448–456. [PubMed: 10449103]

Filippi M, Agosta F. Magnetization transferMRI inmultiple sclerosis. J. Neuroimaging. 2007 Apr; 17(Suppl. 1):22S–26S. [PubMed: 17425730]

Fulton JC, Grossman RI, Udupa J, Mannon LJ, Grossman M, Wei L, et al. MR lesion load and cognitive function in patients with relapsing–remitting multiple sclerosis. AJNR Am. J. Neuroradiol. 1999 Nov-Dec;20(10):1951–1955. [PubMed: 10588124]

Furby J, Hayton T, Anderson V, Altmann D, Brenner R, Chataway J, et al. Magnetic resonance imaging measures of brain and spinal cord atrophy correlate with clinical impairment in secondary progressive multiple sclerosis. Mult. Scler. 2008 Sep; 14(8):1068–1075. [PubMed: 18632782]

Gareau PJ, Rutt BK, Karlik SJ, Mitchell JR. Magnetization transfer and multicomponent T2 relaxation measurements with histopathologic correlation in an experimental model of MS. J. Magn. Reson. Imaging. 2000 Jun; 11(6):586–595. [PubMed: 10862056]

Held U, Heigenhauser L, Shang C, Kappos L, Polman C. Predictors of relapse rate in MS clinical trials. Neurology. 2005 Dec 13; 65(11):1769–1773. [PubMed: 16344520]

Horsfield MA. Magnetization transfer imaging in multiple sclerosis. J. Neuroimaging. 2005; 15(4 Suppl):58S–67S. [PubMed: 16385019]

Kalkers NF, Ameziane N, Bot JC, Minneboo A, Polman CH, Barkhof F. Longitudinal brain volume measurement in multiple sclerosis: rate of brain atrophy is independent of the disease subtype. Arch. Neurol. 2002 Oct; 59(10):1572–1576. [PubMed: 12374494]

Karampekios S, Papanikolaou N, Papadaki E, Maris T, Uffman K, Spilioti M, et al. Quantification of magnetization transfer rate and native T1 relaxation time of the brain: correlation with magnetization transfer ratio measurements in patients with multiple sclerosis. Neuroradiology. 2005 Mar; 47(3):189–196. [PubMed: 15711987]

Kolind SH, Deoni SC. Rapid three-dimensional multicomponent relaxation imaging of the cervical spinal cord. Magn. reson. med. : off.j.Soc. Magn. Reson. Med./Soc. Magn. Reson. Med. 2011 Feb; 65(2):551–556.

Korteweg T, Rovaris M, Neacsu V, Filippi M, Comi G, Uitdehaag BM, et al. Can rate of brain atrophy in multiple sclerosis be explained by clinical and MRI characteristics? Mult. Scler. 2009 Apr; 15(4):465–471. [PubMed: 19091881]

Kurtzke JF. Rating neurologic impairment in multiple sclerosis: an expanded disability status scale (EDSS). Neurology. 1983 Nov; 33(11):1444–1452. [PubMed: 6685237]

NIH-PA Author Manuscript

NIH-PA Author Manuscript

NIH-PA Author Manuscript

Laule C, Vavasour IM, Moore GR, Oger J, Li DK, Paty DW, et al. Water content andmyelinwater fraction inmultiple sclerosis. A T2 relaxation study. J.Neurol. 2004 Mar; 25(3):284–293. [PubMed: 15015007]

Laule C, Leung E, Lis DK, Traboulsee AL, Paty DW, MacKay AL, et al. Myelin water imaging in multiple sclerosis: quantitative correlations with histopathology. Mult. Scler. 2006 Dec; 12(6): 747–753. [PubMed: 17263002]

Lucchinetti C, Bruck W, Parisi J, Scheithauer B, Rodriguez M, Lassmann H. Heterogeneity of multiple sclerosis lesions: implications for the pathogenesis of demyelination. Ann. Neurol. 2000 Jun; 47(6):707–717. [PubMed: 10852536]

MacKay AL, Vavasour IM, Rauscher A, Kolind SH, Madler B, Moore GR, et al. MR relaxation in multiple sclerosis. Neuroimaging Clin N Am. 2009 Feb; 19(1):1–26. [PubMed: 19064196]

Madler B, Drabycz SA, Kolind SH, Whittall KP, MacKay AL. Is diffusion anisotropy an accurate monitor of myelination? Correlation of multicomponent T2 relaxation and diffusion tensor anisotropy in human brain. Magn. Reson. Imaging. 2008 Sep; 26(7):874–888. [PubMed: 18524521]

Mallows C. Some comments on CP. Technometrics. 1973; 15(4):661–675.

Martola J, Stawiarz L, Fredrikson S, Hillert J, Bergstrom J, Flodmark O, et al. Progression of non-age-related callosal brain atrophy in multiple sclerosis: a 9-year longitudinal MRI study representing four decades of disease development. J. Neurol. Neurosurg. Psychiatry. 2007 Apr; 78(4):375–380. [PubMed: 17119006]

Martola J, Bergstrom J, Fredrikson S, Stawiarz L, Hillert J, Zhang Y, et al. A longitudinal observational study of brain atrophy rate reflecting four decades of multiple sclerosis: a comparison of serial 1D, 2D, and volumetric measurements from MRI images. Neuroradiology. 2010 Feb; 52(2):109–117. [PubMed: 19774369]

Mechelli A, Friston KJ, Frackowiak RS, Price CJ. Structural covariance in the human cortex. J. Neurosci. 2005 Sep 7; 25(36):8303–8310. [PubMed: 16148238]

Menon RS, Allen PS. Application of continuous relaxation time distributions to the fitting of data from model systems and excised tissue. Magn. Reson. Med. 1991 Aug; 20(2):214–227. [PubMed: 1775048]

Meyers SM, Laule C, Vavasour IM, Kolind SH, Madler B, Tam R, et al. Reproducibility of myelin water fraction analysis: a comparison of region of interest and voxel-based analysis methods. Magn. Reson. Imaging. 2009 Oct; 27(8):1096–1103. [PubMed: 19356875]

Oh J, Han ET, Pelletier D, Nelson SJ. Measurement of in vivo multi-component T2 relaxation times for brain tissue using multi-slice T2 prep at 1.5 and 3 T. Magn. Reson. Imaging. 2006 Jan; 24(1): 33–43. [PubMed: 16410176]

Oh J, Han ET, Lee MC, Nelson SJ, Pelletier D. Multislice brain myelin water fractions at 3 T in multiple sclerosis. J. Neuroimaging. 2007 Apr; 17(2):156–163. [PubMed: 17441837]

Oouchi H, Yamada K, Sakai K, Kizu O, Kubota T, Ito H, et al. Diffusion anisotropy measurement of brain white matter is affected by voxel size: underestimation occurs in areas with crossing fibers. AJNR Am. J. Neuroradiol. 2007 Jun-Jul;28(6):1102–1106. [PubMed: 17569968]

Papanikolaou N, Papadaki E, Karampekios S, Spilioti M, Maris T, Prassopoulos P, et al. T2 relaxation time analysis in patients with multiple sclerosis: correlation with magnetization transfer ratio. Eur. Radiol. 2004 Jan; 14(1):115–122. [PubMed: 14600774]

Platten M, Ho PP, Youssef S, Fontoura P, Garren H, Hur EM, et al. Treatment of autoimmune neuroinflammation with a synthetic tryptophan metabolite. Science. 2005 Nov 4; 310(5749):850–855. [PubMed: 16272121]

Polman CH, Reingold SC, Edan G, Filippi M, Hartung HP, Kappos L, et al. Diagnostic criteria for multiple sclerosis: 2005 revisions to the “McDonald Criteria”. Ann. Neurol. 2005 Dec; 58(6):840–846. [PubMed: 16283615]

Rudick RA, Fisher E, Lee JC, Simon J, Jacobs L. Use of the brain parenchymal fraction tomeasurewhole brain atrophy in relapsing–remitting MS. Multiple Sclerosis Collaborative Research Group. Neurology. 1999 Nov 10; 53(8):1698–1704. [PubMed: 10563615]

NIH-PA Author Manuscript

NIH-PA Author Manuscript

NIH-PA Author Manuscript

Rudick RA, Lee JC, Nakamura K, Fisher E. Gray matter atrophy correlates with MS disability progression measured with MSFC but not EDSS. J. Neurol. Sci. 2009 Jul 15; 282(1–2):106–111. [PubMed: 19100997]

Schmierer K, Wheeler-Kingshott CA, Boulby PA, Scaravilli F, Altmann DR, Barker GJ, et al. Diffusion tensor imaging of post mortem multiple sclerosis brain. NeuroImage. 2007 Apr 1; 35(2): 467–477. [PubMed: 17258908]

Seewann A, Vrenken H, van der Valk P, Blezer EL, Knol DL, Castelijns JA, et al. Diffusely abnormal white matter in chronic multiple sclerosis: imaging and histopathologic analysis. Arch. Neurol. 2009 May; 66(5):601–609. [PubMed: 19433660]

Smith, S.; Jenkinson, M. FSLUTILS. 2000. http://wwwfmriboxacuk/fsl/avwutils/indexhtml2000

Smith SM, Jenkinson M, Woolrich MW, Beckmann CF, Behrens TE, Johansen-Berg H, et al. Advances in functional and structural MR image analysis and implementation as FSL. NeuroImage. 2004; 23(Suppl. 1):S208–S219. [PubMed: 15501092]

Song SK, Sun SW, Ju WK, Lin SJ, Cross AH, Neufeld AH. Diffusion tensor imaging detects and differentiates axon and myelin degeneration in mouse optic nerve after retinal ischemia. NeuroImage. 2003 Nov; 20(3):1714–1722. [PubMed: 14642481]

Sormani MP, Bruzzi P, Beckmann K, Wagner K, Miller DH, Kappos L, et al. MRI metrics as surrogate endpoints for EDSS progression in SPMS patients treated with IFN beta-1b. Neurology. 2003 May 13; 60(9):1462–1466. [PubMed: 12743232]

vanWaesberghe JH, Kamphorst W, De Groot CJ, vanWalderveen MA, Castelijns JA, Ravid R, et al. Axonal loss in multiple sclerosis lesions: magnetic resonance imaging insights into substrates of disability. Ann. Neurol. 1999 Nov; 46(5):747–754. [PubMed: 10553992]

Vavasour IM, Whittall KP, MacKay AL, Li DK, Vorobeychik G, Paty DW. A comparison between magnetization transfer ratios and myelin water percentages in normals and multiple sclerosis patients. Magn. Reson. Med. 1998 Nov; 40(5):763–768. [PubMed: 9797161]

Vavasour IM, Clark CM, Li DK, Mackay AL. Reproducibility and reliability ofMR measurements in white matter: clinical implications. NeuroImage. 2006 Aug 15; 32(2):637–642. [PubMed: 16677833]

Vellinga MM, Geurts JJ, Rostrup E, Uitdehaag BM, Polman CH, Barkhof F, et al. Clinical correlations of brain lesion distribution in multiple sclerosis. J. Magn. Reson. Imaging. 2009 Apr; 29(4):768–773. [PubMed: 19306365]

Vrenken H, Seewann A, Knol DL, Polman CH, Barkhof F, Geurts JJ. Diffusely abnormal white matter in progressive multiple sclerosis: in vivo quantitative MR imaging characterization and comparison between disease types. AJNR Am. J. Neuroradiol. 2010 Mar; 31(3):541–548. [PubMed: 19850760]

Webb S, Munro CA, Midha R, Stanisz GJ. Is multicomponent T2 a goodmeasure of myelin content in peripheral nerve? Magn. Reson. Med. 2003 Apr; 49(4):638–645. [PubMed: 12652534]

Weiner HL. The challenge of multiple sclerosis: how do we cure a chronic heterogeneous disease? Ann. Neurol. 2009 Mar; 65(3):239–248. [PubMed: 19334069]

Whittall KP, MacKay AL, Graeb DA, Nugent RA, Li DK, Paty DW. In vivo measurement of T2 distributions and water contents in normal human brain. Magn. Reson. Med. 1997 Jan; 37(1):34–43. [PubMed: 8978630]

Yushkevich PA, Piven J, Hazlett HC, Smith RG, Ho S, Gee JC, et al. Userguided 3D active contour segmentation of anatomical structures: significantly improved efficiency and reliability. NeuroImage. 2006 Jul 1; 31(3):1116–1128. [PubMed: 16545965]

Zivadinov R. Advanced magnetic resonance imaging metrics: implications for multiple sclerosis clinical trials. Methods Find. Exp. Clin. Pharmacol. 2009 Jan-Feb;31(1):29–40. [PubMed: 19357796]

NIH-PA Author Manuscript
NIH-PA Author Manuscript
NIH-PA Author Manuscript

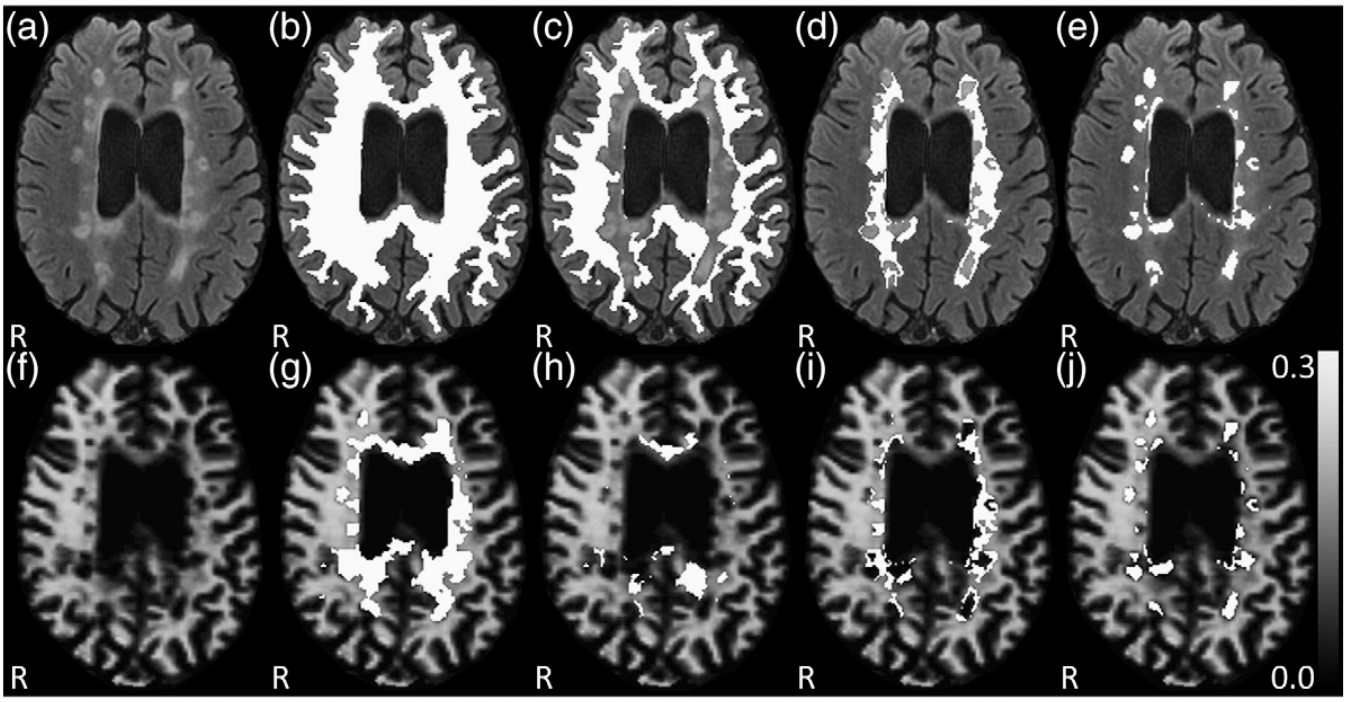

Fig. 1.

WM segmentation and voxel-based analysis in a SPMS patient. (a) native FLAIR image, (b) superimposed WM mask, (c) NAWM, (d) DAWM, (e) T2 lesion segmentation mask, and (lower row) deficient MWF voxel masks within specific WM regions projected onto the MWF map with (f) the native MWF map, (g) DV in total WM, (h) DV in NAWM, (i) DV in DAWM, and (j) DV in T2 lesions.

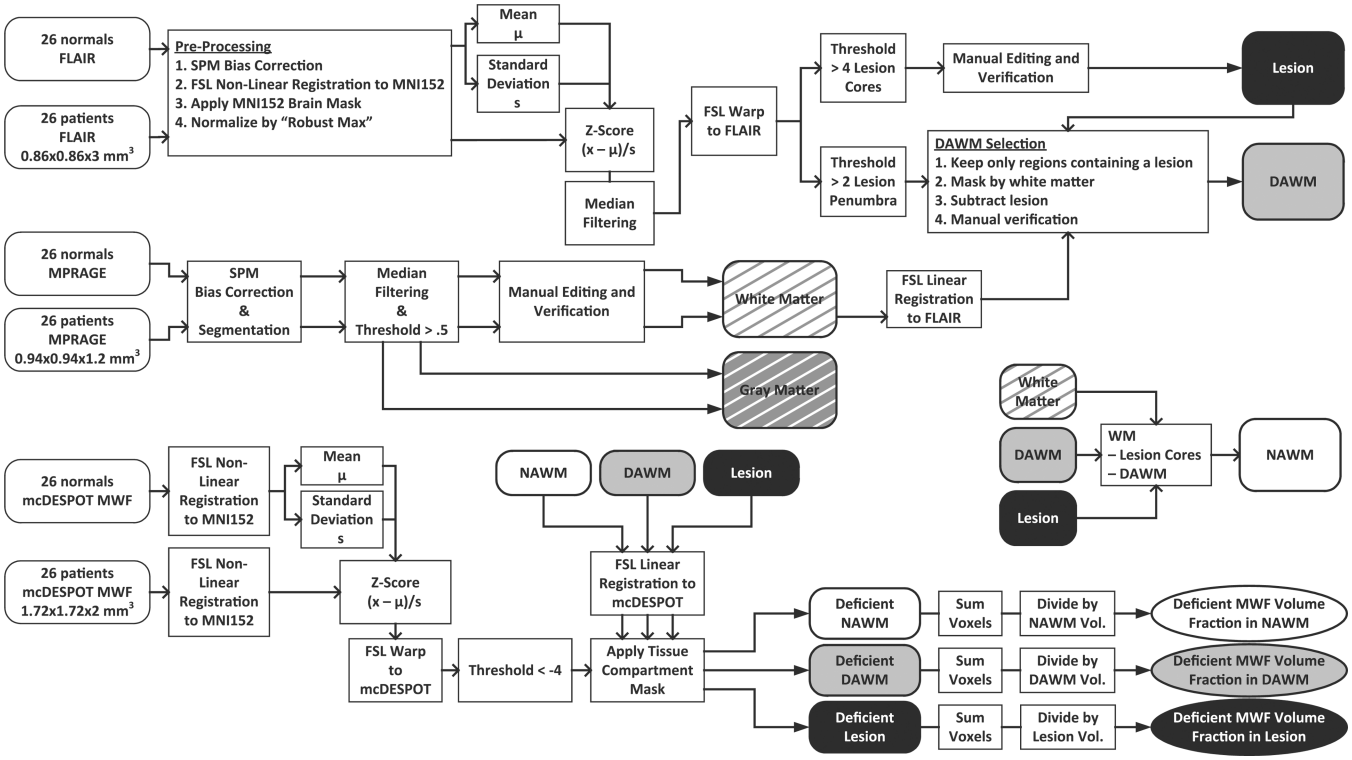

Fig. 2.

Data processing graphical display. Workflow of image data post-processing including the mcDESPOT analysis based MWF map generation, WM mask creation, region segmentation processes, and deficient MWF map creation based on the study population in MNI standard space, finally resulting in region-specific maps.

NIH-PA Author Manuscript NIH-PA Author Manuscript NIH-PA Author Manuscript

NIH-PA Author Manuscript

NIH-PA Author Manuscript

NIH-PA Author Manuscript

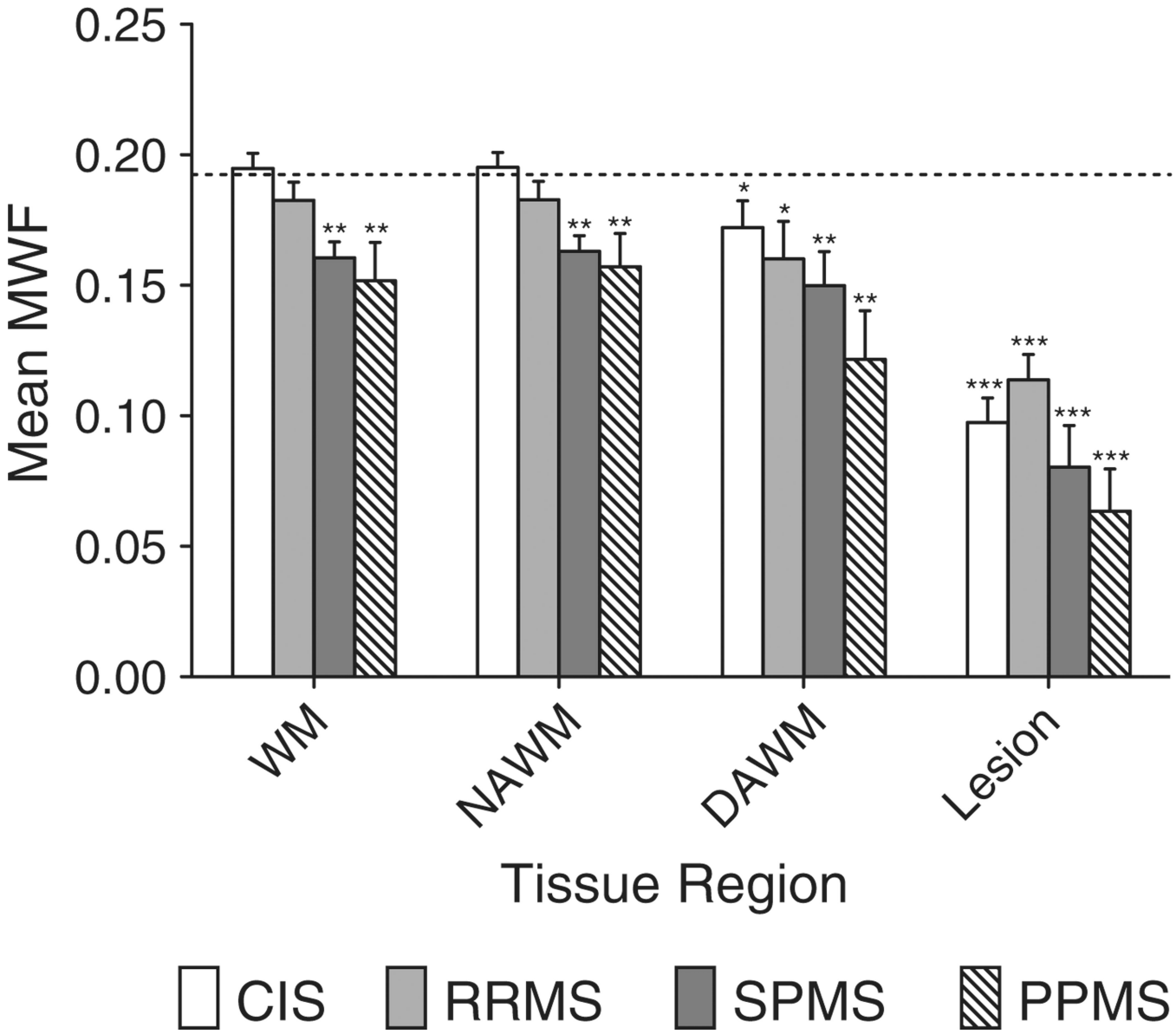

Fig. 3.

Mean myelin water fraction in white matter regions in different MS courses and healthy controls. The dotted line shows mean MWF in WM for healthy controls. Rank sum testing was done for each bar against this value. Testing was also done for RRMS vs. SPMS and CIS vs. RRMS, and any significant differences shown with connecting bracket. Significance levels: * $p < 0.05$, ** $p < 0.01$, *** $p < 0.001$.

NIH-PA Author Manuscript
NIH-PA Author Manuscript
NIH-PA Author Manuscript

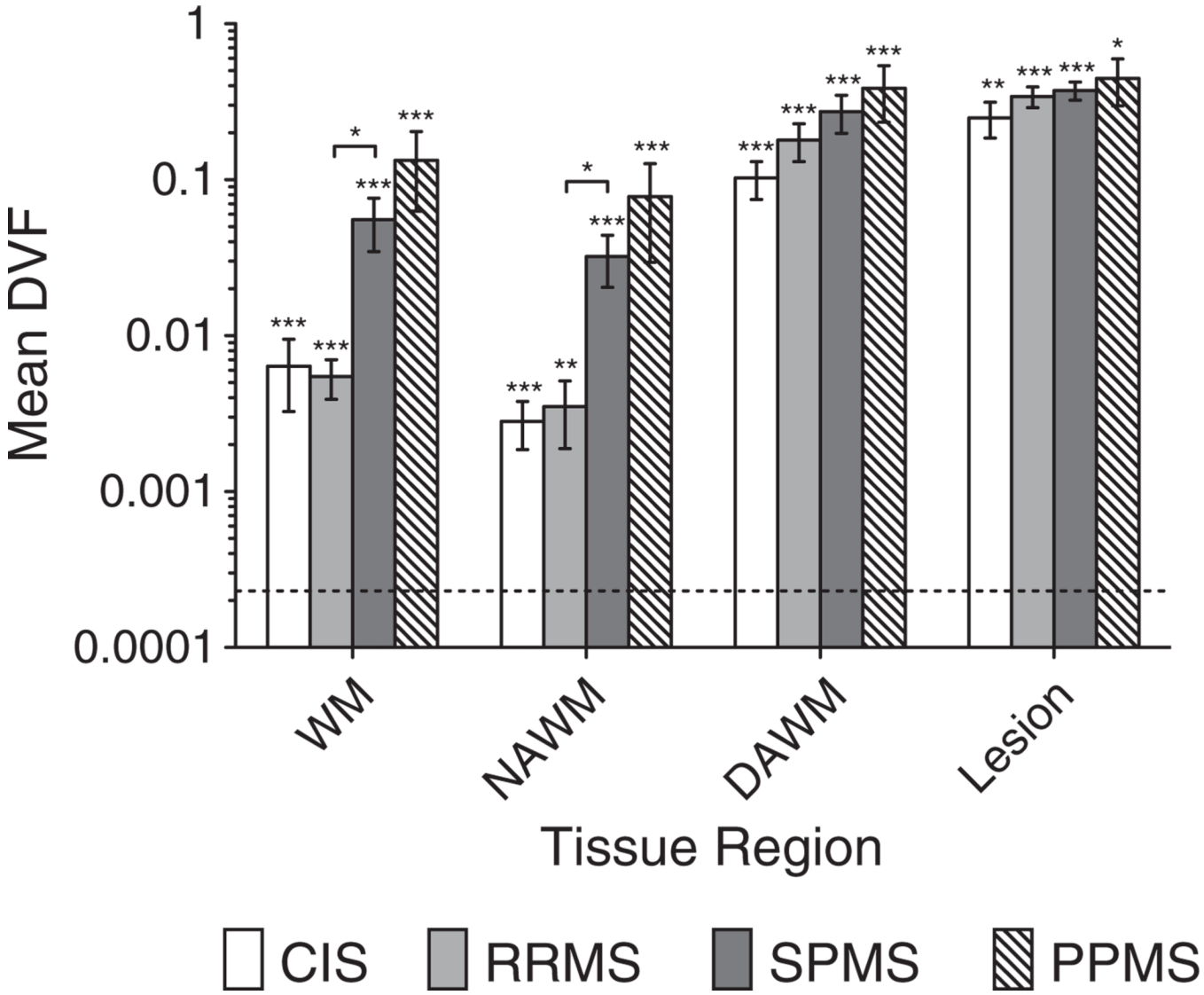

Fig. 4.

The fraction of each WM region that has deficient MWF in different MS courses and healthy controls. The dotted line shows mean DVF in WM for healthy controls. All patient subclasses were significantly different from healthy controls. Rank sum testing was done for each bar against this value. Testing was also done for RR vs. SP and CIS vs. RR, and any significant differences shown with connecting bracket. Significance levels: * $p < 0.05$, ** $p < 0.01$, *** $p < 0.001$.

NIH-PA Author Manuscript
NIH-PA Author Manuscript
NIH-PA Author Manuscript

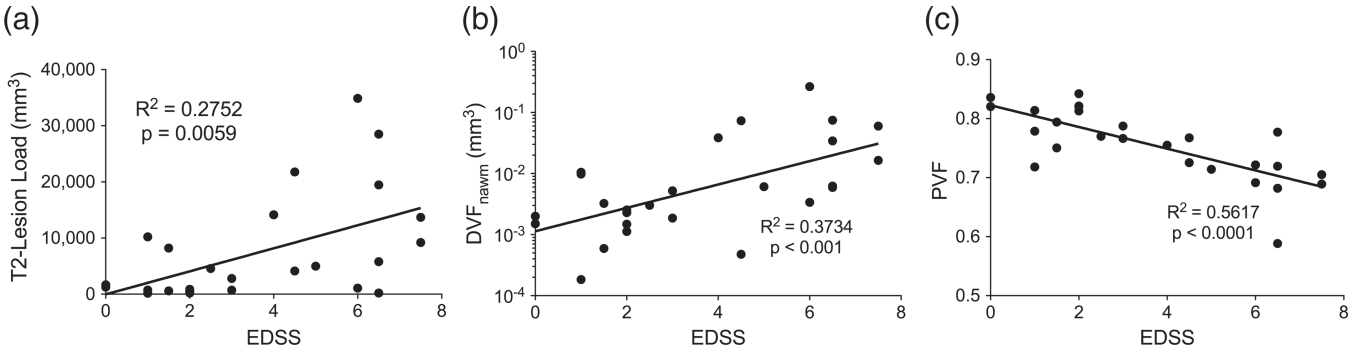

Fig. 5.

(a) T2-lesion-load (total T2 lesion volume) vs. EDSS, (b) deficient MWF volume fraction in NAWM (DVF_{NAWM}) with a log transform applied to improve linearity vs. EDSS, and (c) parenchymal volume fraction (PVF) vs. EDSS.

NIH-PA Author Manuscript
NIH-PA Author Manuscript
NIH-PA Author Manuscript

Table 1

Demographic data of patients with MS and healthy controls.

Demographic data	Healthy controls	All pat	CIS	RRMS	SPMS	PPMS
N	26	26	10	5	6	5
Median age, year (interquartile range)	43 (20)	52 (17)	42 (20)	41 (20)	56 (13)	55 (10)
Male/female ratio	10/16	7/19	3/7	0/5	0/6	4/1
Median disease duration, year (IQR)	–	11 (18)	2 (3)	12 (10)	29 (14)	18 (9)
Median EDSS score (IQR)	–	3.0 (4.5)	1.75 (1.0)	2.0 (2.25)	6.5 (1.5)	6.0 (1.75)

Neuroimage. Author manuscript; available in PMC 2013 June 05.

NIH-PA Author Manuscript NIH-PA Author Manuscript NIH-PA Author Manuscript

Table 2

Mean WM region volume (mm^3), mean myelin water fraction (MWF), mean deficient MWF volume fraction (DVF) and their standard deviations (SD) in specific WM regions and different MS courses. Rank sum testing was performed against the MWF or DVF in total WM for healthy controls.

	Mean WM region volume [mm^3] (SD) | Mean MWF (SD) | Mean DVF (SD)											
	Total WM			**NAWM**			**DAWM**			**T2 lesions**		
Healthy controls	4.72E5 (5.52E4)	0.192 (0.015)	0.0002 (0.0004)	–	–	–	–	–	–	–	–	–
All patients	4.47E5 (7.52E4)	0.176 * (0.026)	0.042 *** (0.084)	4.28E5 (8.53E4)	0.178 * (0.024)	0.024 *** (0.054)	1.34E4 (1.61E4)	0.155 *** (0.037)	0.212 *** (0.205)	7.39E3 (9.50E3)	0.090 *** (0.035)	0.334 *** (0.209)
CIS	4.70E5 (8.47E4)	0.195 (0.018)	0.006 *** (0.010)	4.62E5 (8.87E4)	0.195 (0.018)	0.003 *** (0.003)	6.09E3 (9.11E3)	0.172 * (0.032)	0.103 *** (0.088)	2.57E3 (3.70E3)	0.097 *** (0.030)	0.249 ** (0.204)
RRMS	4.36E5 (5.16E4)	0.183 (0.016)	0.006 *** (0.004)	4.32E5 (4.06E3)	0.183 (0.016)	0.004 ** (0.004)	2.56E3 (4.06E3)	0.160 * (0.032)	0.180 *** (0.109)	2.34E3 (1.96E3)	0.114 ** (0.022)	0.342 *** (0.115)
SPMS	4.35E5 (6.55E4)	0.161 ** (0.015)	0.055 *** (0.051)	4.09E5 (7.71E4)	0.163 ** (0.015)	0.032 *** (0.029)	1.81E4 (1.07E4)	0.150 ** (0.032)	0.274 *** (0.185)	1.19E4 (8.03E3)	0.080 *** (0.039)	0.374 *** (0.123)
PPMS	4.27E5 (9.47E4)	0.152 ** (0.033)	0.133 *** (0.157)	3.81E5 (1.08E5)	0.157 ** (0.028)	0.078 *** (0.108)	3.35E4 (2.12E4)	0.122 ** (0.042)	0.386 *** (0.341)	1.67E4 (1.49E4)	0.063 *** (0.036)	0.447 * (0.334)

Significance levels:

* $p < 0.05$,

** $p < 0.01$,

*** $p < 0.001$.